

Geophysical Research Letters®

RESEARCH LETTER

10.1029/2021GL097371

Key Points:

- Aeromagnetic analysis reveals basement surface and evidence of fault-controlled extensional basins beneath Antarctica's Ross Ice Shelf (RIS)
- Active faults at Siple Coast likely influence ice streams through control of geothermal heat, groundwater, and glacioisostatic adjustments
- A basement high beneath RIS spatially coincides with a lithospheric boundary, with contrasting sedimentary basins on either side

Supporting Information:

Supporting Information may be found in the online version of this article.

Correspondence to:

M. D. Tankersley,
matthew.tankersley@vuw.ac.nz

Citation:

Tankersley, M. D., Horgan, H. J., Siddoway, C. S., Caratori Tontini, F., & Tinto, K. J. (2022). Basement topography and sediment thickness beneath Antarctica's Ross Ice Shelf. *Geophysical Research Letters*, 49, e2021GL097371. <https://doi.org/10.1029/2021GL097371>

Received 6 DEC 2021

Accepted 5 MAY 2022

Basement Topography and Sediment Thickness Beneath Antarctica's Ross Ice Shelf



M. D. Tankersley^{1,2} , H. J. Horgan¹ , C. S. Siddoway³ , F. Caratori Tontini^{2,4} , and K. J. Tinto⁵

¹Antarctic Research Centre, Victoria University of Wellington, Wellington, New Zealand, ²GNS Science, Lower Hutt, New Zealand, ³Colorado College, Colorado Springs, CO, USA, ⁴University of Genova, Genova, Italy, ⁵Lamont-Doherty Earth Observatory, Columbia University, Palisades, NY, USA

Abstract New geophysical data from Antarctica's Ross Embayment reveal the structure and subglacial geology of extended continental crust beneath the Ross Ice Shelf. We use airborne magnetic data from the ROSETTA-Ice Project to locate the contact between magnetic basement and overlying sediments. We delineate a broad, segmented basement high with thin (0–500m) non-magnetic sedimentary cover which trends northward into the Ross Sea's Central High. Before subsiding in the Oligocene, this feature likely facilitated early glaciation in the region and subsequently acted as a pinning point and ice flow divide. Flanking the high are wide sedimentary basins, up to 3700m deep, which parallel the Ross Sea basins and likely formed during Cretaceous-Neogene intracontinental extension. NW-SE basins beneath the Siple Coast grounding zone, by contrast, are narrow, deep, and elongate. They suggest tectonic divergence upon active faults that may localize geothermal heat and/or groundwater flow, both important components of the subglacial system.

Plain Language Summary The bedrock geology of Antarctica's southern Ross Embayment is concealed by 100–1000s of meters of sedimentary deposits, seawater, and the floating Ross Ice Shelf (RIS). Our research strips away those layers to discover the shape of the consolidated bedrock below, which we refer to as the basement. To do this, we use the contrast between non-magnetic sediments and magnetic basement rocks to map out the depth of the basement surface under the RIS. Our primary data source is airborne measurements of the variation in Earth's magnetic field across the ice shelf, from flight lines spaced 10-km apart. We use the resulting basement topography to highlight sites of possible influence upon the Antarctic Ice Sheet and to further understand the tectonic history of the region. We discover contrasting basement characteristics on either side of the ice shelf, separated by a N-S trending basement high. The West Antarctic side displays evidence of active faults, which may localize geothermal heat, accommodate movements of the solid earth caused by changes in the size of the Antarctic Ice Sheet, and control the flow of groundwater between the ice base and aquifers. This work addresses critical interactions between ice and the solid earth.

1. Introduction

The southern sector of Antarctica's Ross Embayment beneath the Ross Ice Shelf (RIS; area ~480,000 km²) is poorly resolved because the region is not accessible to conventional seismic or geophysical surveying. Rock exposures on land suggest that Ross Ice Shelf (RIS) crust consists of early Paleozoic post-orogenic sediments, intruded in places by mid-Paleozoic and Cretaceous granitoids (Goodge, 2020; Luyendyk et al., 2003). Following the onset of extension in the mid-Cretaceous, grabens formed and filled with terrestrial and marine deposits, continuing into the Cenozoic (e.g., Coenen et al., 2019; Sorlien et al., 2007), as the Ross Embayment underwent thermal subsidence (Karner et al., 2005; Wilson & Luyendyk, 2009). The physiography of this region then responded to the onset of glaciation in the Oligocene (Paxman et al., 2019), coinciding with localized extension in the western Ross Sea until 11 Ma (Granot & Dyment, 2018). The Oligocene-early-Miocene paleo-landscape of the Ross Sea sector was revealed by marine seismic data (e.g., Brancolini et al., 1995; Pérez et al., 2021) and offshore drilling that penetrated crystalline basement (DSDP Site 270; Ford & Barrett, 1975) (Figure 1). Recognition of the role of elevated topography in Oligocene formation of the Antarctic Ice Sheet (DeConto & Pollard, 2003; Wilson et al., 2013) and the likely influence of subglacial topography upon ice sheet processes during some climate states (Austermann et al., 2015; Colleoni et al., 2018) motivated our effort to determine basement topography beneath the RIS.

© 2022 The Authors.

This is an open access article under the terms of the [Creative Commons Attribution-NonCommercial License](#), which permits use, distribution and reproduction in any medium, provided the original work is properly cited and is not used for commercial purposes.

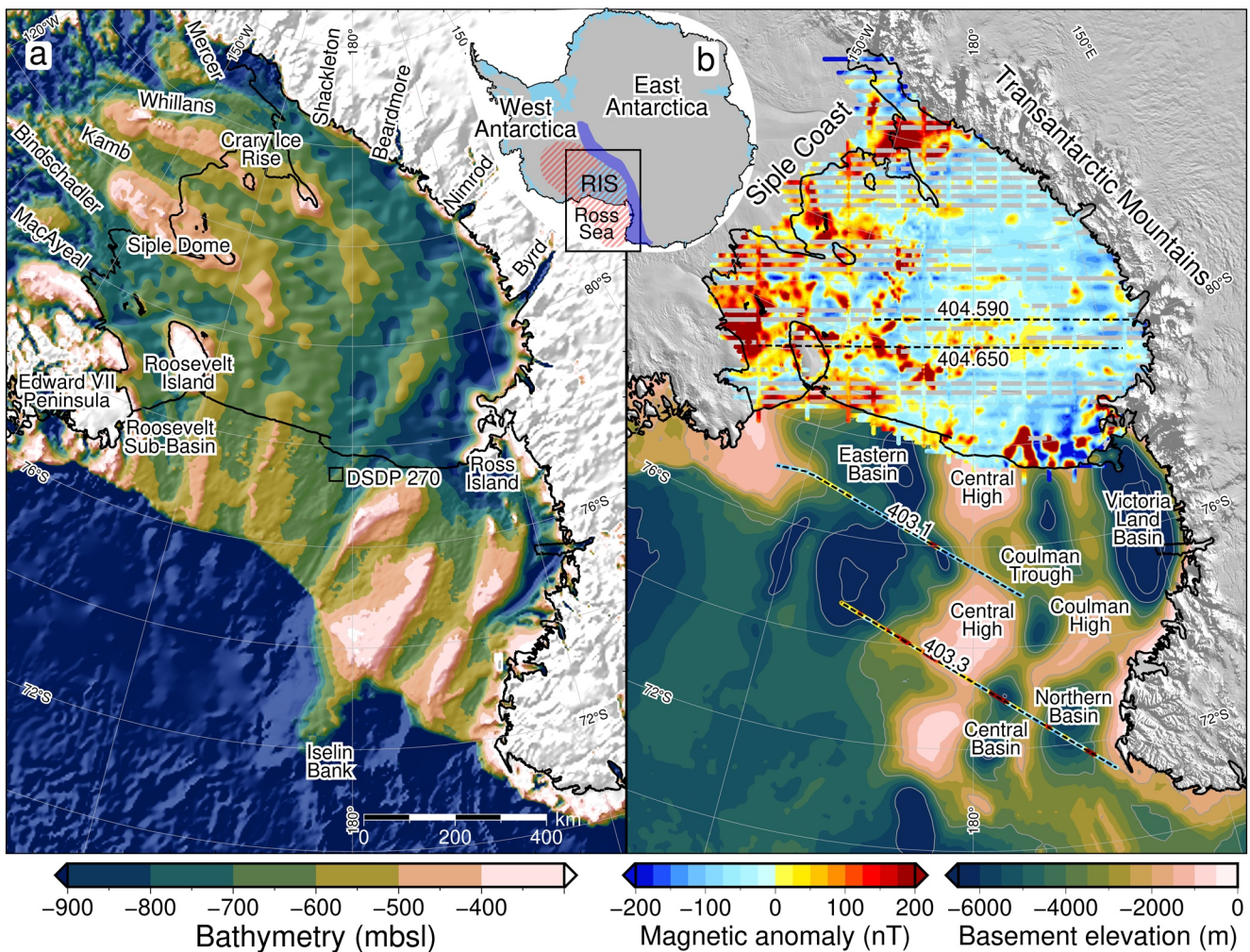


Figure 1. (a) Bathymetry and sub-ice bed elevations (Morlighem et al., 2020) including ROSETTA-Ice gravity-derived bathymetry (Tinto et al., 2019) beneath the Ross Ice Shelf (RIS). Labels include ice streams and outlet glaciers. (b) Basement elevation from Antarctic Offshore Stratigraphy project marine seismic compilation in the Ross Sea (Brancolini et al., 1995) and airborne magnetic data from ROSETTA-Ice (over RIS) and Operation IceBridge (black dashed lines). Inset map shows figure location, West Antarctic Rift System (hatched red), Transantarctic Mountains (dark blue), and ice shelves (light blue). Shelf edge, grounding line, and coastlines in black (Rignot et al., 2013). MODIS imagery from Scambos et al. (2007).

Ice sheet dynamics are of high interest in the RIS region because its grounding zone (GZ) and pinning points (Still et al., 2019) buttress Antarctica's second-largest drainage basin (Tinto et al., 2019). Our work in this sensitive region seeks to delimit the extent and geometry of competent basement because the margins of basement highs are sites of strong contrasts in permeability that influence the circulation of subglacial waters. A spectacular example of the confinement of subglacial water between the ice sheet and basement exists in ice radar profiles for the continental interior (Bell et al., 2011), but little is known about the subglacial hydrology of deep groundwater reservoirs within sediment-filled marine basins that receive terrestrial freshwater influx (Gustafson et al., 2022; Siegert et al., 2018). These basins may contain up to 50% of total subglacial freshwater (Christoffersen et al., 2014), where the discharge and recharge along fault-damage zones (Jolie et al., 2021) is controlled by pressure from the overriding ice sheet (Gooch et al., 2016). Possible evidence that RIS basement margins localize basal waters, causing the advection of geothermal heat, comes from elevated values and significant spatial variability of measured geothermal heat flux (GHF) at points around the Ross Embayment (Begeman et al., 2017). Here we present the first map of magnetic basement topography and thickness of overlying non-magnetic sediments for the southern Ross Embayment, developed using ROSETTA-Ice (2015–2019) airborne magnetic data (Figure 1b, Tinto et al., 2019). Our work reveals three major sedimentary basins and a broad basement ridge that separates crust of contrasting basement characteristics.

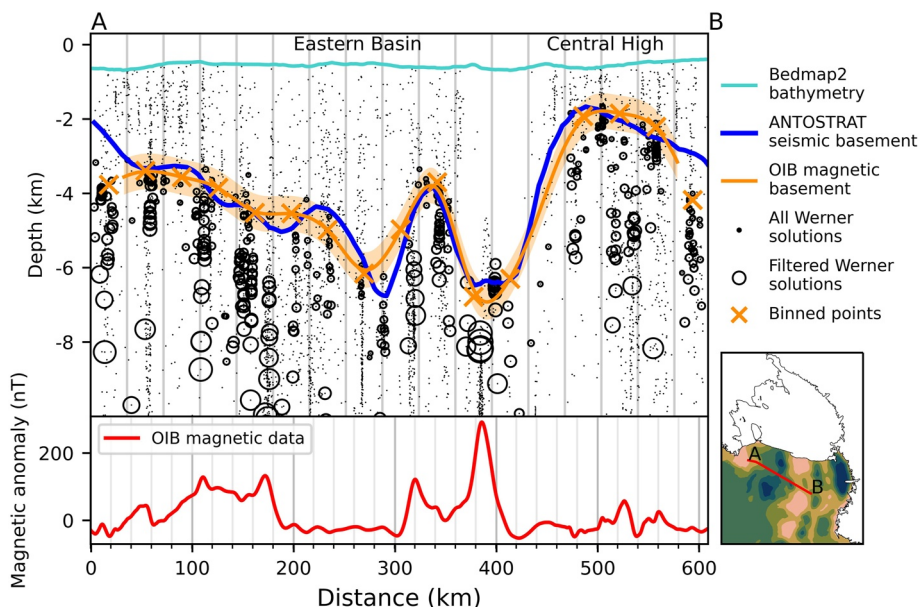


Figure 2. Ross Sea magnetic and seismic basement comparison. Operation IceBridge airborne magnetic data (lower panel) from segment 403.1 used in Werner deconvolution to produce magnetic anomaly source solutions (black dots). Filtering removed shallow solutions, and remaining solutions (circles scaled to magnetic susceptibility) were binned and interpolated to produce the magnetic basement (orange line with uncertainty band).

2. Data and Methods

We use ROSETTA-Ice aeromagnetic data to image the shallowest magnetic signals in the crust. Assuming that the overlying sediments and sedimentary rocks produce smaller magnetic anomalies than the crystalline basement, we treat the resulting solutions as the depth to the magnetic basement (Text S1 in Supporting Information S1). To do this, we implemented Werner deconvolution (Werner, 1953) on 2D moving and expanding windows of line data, isolating anomalies and solving for their source parameters (Text S2 in Supporting Information S1, location, depth, susceptibility, body type). The resulting solutions are non-unique; each observed magnetic anomaly can be solved by bodies at multiple locations and depths by varying the source's magnetic susceptibility and width. The result is a depth scatter of solutions (Figures 2 and S2 in Supporting Information S1), which tend to vertically cluster beneath the true source. This magnetic basement approach has been used to map sedimentary basins throughout Antarctica (i.e., Bell et al., 2006; Frederick et al., 2016; Karner et al., 2005; Studinger et al., 2004) where typically, the tops of solution clusters are manually selected to represent the basement depth. Our approach expands on this method by utilizing a reliable, automated method of draping a surface over these depth-scattered solutions to produce a continuous basement surface (Text S3 and S4 in Supporting Information S1).

We implemented a 2-step tuning process that ties our RIS magnetic basement to well-constrained seismic basement in the Ross Sea, from the Antarctic Offshore Stratigraphy project (ANTOSTRAT) (Figure 1b, Brancolini et al., 1995). This involved using Operation IceBridge (OIB) airborne magnetic data (Cochran et al., 2014) collected over the RIS and Ross Sea. Minimizing misfits between OIB magnetic basement and ANTOSTRAT basement, as well as between OIB and ROSETTA-Ice magnetic basements, enabled tuning of our method to optimal basement depths (Figures 2, S2, S3e, and S3f, Text S3 and S4 in Supporting Information S1).

Our RIS results (Figure S4 in Supporting Information S1) were merged with offshore ANTOSTRAT data (Brancolini et al., 1995) and smoothed with an 80 km Gaussian filter to match the characteristic wavelengths of the Ross Sea basement (Text S5 in Supporting Information S1). The combined grid (Figure 3a) was then subtracted from BedMachine bathymetry (Figure 1a, Text S6 in Supporting Information S1, Morlighem et al., 2020), to obtain the sediment thickness distribution for the Ross Embayment (Figure 3b).

These sub-RIS results together with free-air gravity data allowed us to infer the locations of regional scale faults beneath the RIS. Criteria used to locate faults include (a) high relief on the magnetic basement surface, (b) linear

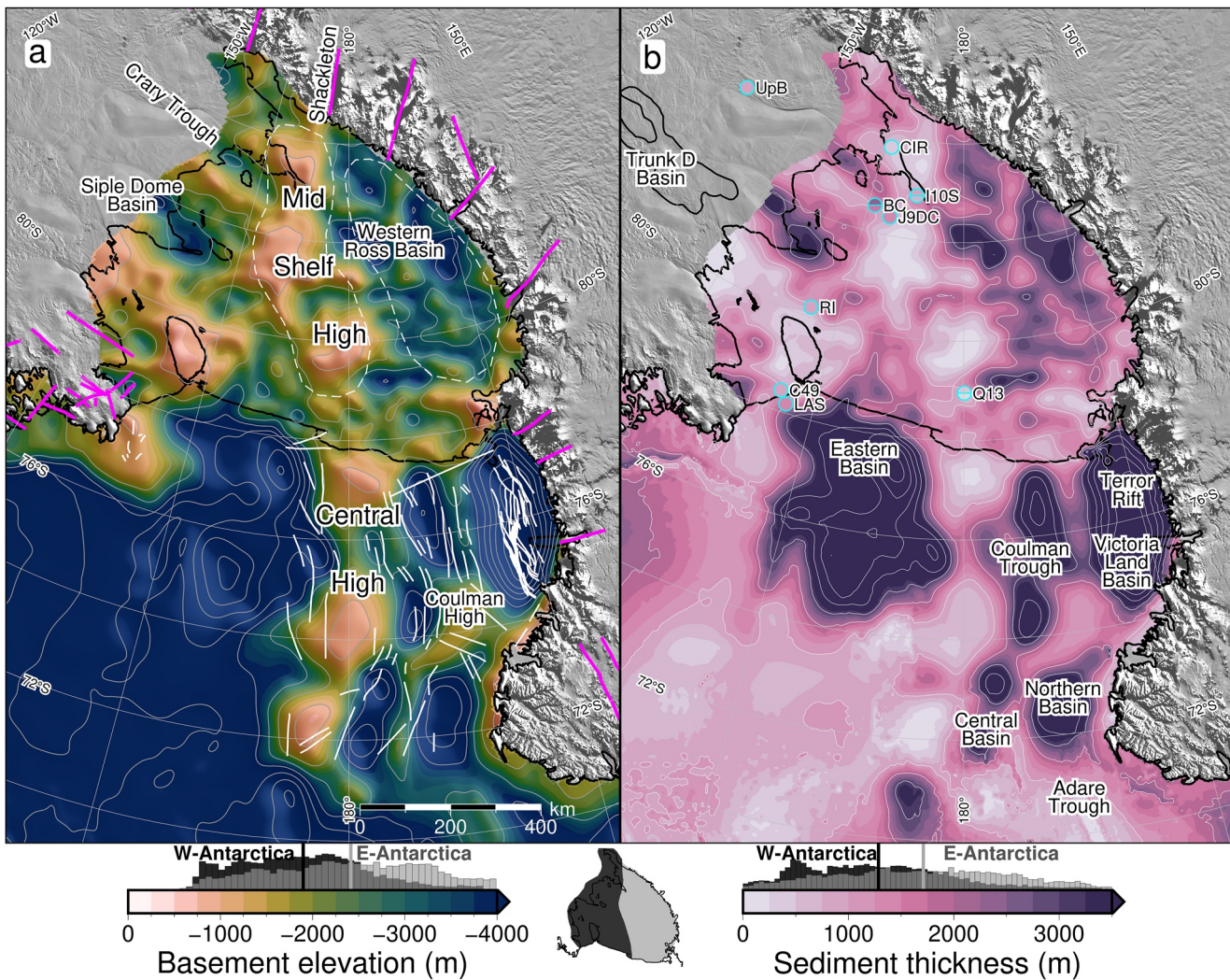


Figure 3. (a) Basement elevation (magnetic for Ross Ice Shelf (RIS), seismic elsewhere) contoured at 1 km intervals. Pink lines are onshore mapped and inferred faults (Ferraccioli et al., 2002; Goodge, 2020; Siddoway, 2008). White lines are offshore faults (Chiappini et al., 2002; Luyendyk et al., 2001; Salvini et al., 1997; Sauli et al., 2021). Dashed white lines show Mid Shelf High and Western Ross Basin extents. (b) Sediment thickness contoured at 1 km intervals. Previous basement-imaging RIS seismic surveys (cyan circles, Table S1 in Supporting Information S1) are plotted on same color scale, with upper and lower uncertainty ranges as circle halves, where reported. Trunk D Basin outlined in West Antarctica (Bell et al., 2006). Color scales for both (a and b) are set to sub-RIS data range. Colorbar histograms show data distribution for East versus West Antarctic sides of the sub-RIS, separated by the Mid-Shelf High. Inset map shows East versus West divide. Vertical lines on histograms denote average values of each side.

trends that cross zones of shallow basement, (c) high gradient gravity anomalies (Figure S1a in Supporting Information S1, ROSETTA-Ice) and (d) large contrasts in sediment thickness. Narrow, deep, linear basins are likely to be controlled by active faults (e.g., Drenth et al., 2019; Finn, 2002). We display the inferred faults upon a base map of crustal stretching factors (β -factor; the ratio of crustal thickness before and after extension, Figure 4a), using an initial crustal thickness of 38 km (Müller et al., 2007), a continent-wide Moho model (An et al., 2015), and our basement surface as the top of the crust (Text S6 in Supporting Information S1).

3. Results

We find that an almost continuous drape of sediment covers the RIS region (Figure 3b), with only ~3% of the area having <200 m of sedimentary cover. Prominent beneath the midline of the RIS is a broad NNW-SSE trending basement ridge (Figure 3a, Mid-Shelf High; MSH), which comprises most of the shallowest (<700 m below sea level (mbsl)) sub-RIS basement, with several regions with as little as 100 m of sedimentary cover. Basement is

deeper on the East Antarctic side of the MSH, where it averages \sim 2,400 mbsl, compared to an average depth of \sim 1,900 mbsl on the West Antarctic side (Figure 3a histogram). Sedimentary fill is \sim 400m greater and more uniformly distributed on the East Antarctic side than the West Antarctic side (Figure 3b histogram).

To estimate our uncertainty (Text S7 in Supporting Information S1), we examined the misfit between OIB and ANTOSTRAT basement (Figures 2 and S2 in Supporting Information S1) and between our basement and OIB basement (Figures S3e and S3f in Supporting Information S1). There is a median misfit of 480m (22% of average RIS depth) for basement (Figures S5 and S6 in Supporting Information S1). A similar 470m median basement misfit is estimated by comparing our results to eight active source seismic surveys (Figure 3b, Table S1 in Supporting Information S1). Incorporating the \sim 70m uncertainty in the bathymetry model (Tinto et al., 2019), our representative sediment thickness uncertainty is 550m (37% of average RIS thickness, Figure S5 in Supporting Information S1).

A single broad and deep basin (300×600 km) separates the MSH and the Transantarctic Mountains (TAM) (Figure 3a, Western Ross Basin). The Western Ross Basin parallels the TAM and has the deepest-observed sub-RIS basement depths of 4,500 mbsl, accommodating sediments up to 3800m thick (Figure 3b). It contains a long, narrow NW-SE trending ridge with \sim 1500m structural relief above the basement sub-basins on either side. Bordering the MSH on the east, an elongate NW-SE trending basin runs from the RIS calving front to the Siple Coast GZ (Figure 3a), where beneath Siple Dome we discover a 100×200 km depocenter reaching basement depths up to 4,000 mbsl, with sediments up to 3700m thick. We refer to this depocenter as Siple Dome Basin, a feature bounded on the east by a basement high that trends southward from Roosevelt Island. This high rises to its shallowest point at the GZ, where its sedimentary cover is less than 100m. A second deep, narrow basin (50×200 km in dimension) is found along the north margin of Crary Ice Rise, separated from the Siple Dome Basin by a NW-SE ridge underlying Kamb Ice Stream. The basin, labeled Crary Trough in Figure 3a, reaches basement depths of 3,200 mbsl, with sediments 1800–2700m thick. The southernmost RIS has an additional depocenter with up to 2000m of fill beneath Whillans Ice Stream (location in Figure 1a).

Inferred active sub-RIS faults (Figures 4a and S1 in Supporting Information S1) correspond to narrow, linear basement basins with high-gradient gravity anomalies, prevalent on the West Antarctic side (Figure S1a in Supporting Information S1). Inactive normal and strike-slip faults are inferred along lineaments that segment the shallow MSH into blocks and are oriented parallel to TAM outlet glacier faults. β -factors are indicative of thinned crust and are different on either side of the MSH. The TAM side shows higher β -factors (average 1.99) with low variability. The West Antarctic side has lower β -factors overall (average 1.82), but with some higher values up to 2.1 (Figure 4a).

4. Discussion

Sub-RIS sedimentary basins align with and show lateral continuity with the Ross Sea's Roosevelt Sub-Basin, Eastern Basin, Coulman Trough, and Victoria Land Basin (Figure 3, e.g., Cooper et al., 1995). The MSH passes northward into the Ross Sea's prominent Central High (CH). At the southern RIS margin, the narrow Siple Dome Basin has continuity with the previously identified Trunk D Basin (Figure 3a, Bell et al., 2006). The throughgoing trends imply regional continuity of crustal structure and a common tectonic development of the Ross Sea and RIS regions. Our sediment thicknesses are compatible with those determined by (a) eight active-source seismic surveys (Figure 3b), for which the median misfit is 470m (Table S1 in Supporting Information S1), and (b) surface wave dispersion indicating 2–4 km of sediment under the RIS, similar to our range, with the maximum beneath Crary Ice Rise (Zhou et al., 2022). Three additional western RIS seismic profiles report up to several kilometers of sediment, in general accordance with our results (Beaudoin et al., 1992; Stern et al., 1991; ten Brink et al., 1993). Additionally, machine learning applied to geophysical datasets predicts a high likelihood of sedimentary basins at the locations of Siple Dome Basin and Crary Trough (L. Li et al., 2021).

4.1. West Antarctic Rift System Extensional Basins

The Western Ross Basin has a configuration similar to the western Ross Sea rift basins (e.g., Salvini et al., 1997) with a broad and deep basin, separated into distinct depocenters by a linear, low relief ridge. The deeper of the

depocenters, on the TAM side of the ridge, coincides with alternating high and low free-air gravity anomalies (Figure S1a in Supporting Information S1). These similarities suggest the sub-RIS continuations of Coulman Trough and Victoria Land Basin (Figure 3b) likely share a common tectonic origin as fault-controlled basins (Figures 3a and 4a) formed through Cretaceous distributed continental extension across the WARS (Jordan et al., 2020). These sub-RIS basins terminate against the southern segment of the MSH (Figure 3a).

The linear ridge within the Western Ross Basin (Figure 3a) may be an expression of normal or oblique faults linked to the southward-narrowing Terror Rift (Sauli et al., 2021), formed due to Cenozoic oceanic spreading in the Adare Trough (Figure 3b, Granot & Dymant, 2018). The Western Ross Basin, with up to 3800m of fill, terminates along the prominent edge of the MSH that lines up with the fault-controlled trough and crustal boundary that passes southward beneath Shackleton Glacier (Borg et al., 1990). We interpret the basement lineament (Figure 4a) as a transfer fault separating sectors of crust extended to different degrees.

The southeastern RIS margin is distinguished by linear ridges and narrow, deep basins. The prominent NW-SE basement trends coincide with high-gradient gravity anomalies (Figure S1a in Supporting Information S1, Tinto et al., 2019) and thick sediments, suggesting normal fault control and active divergent tectonics beneath the GZ. Our Siple Coast cross-section (Figure 4b) displays dramatic basement relief, exceeding 2 km, in the Siple Dome Basin and Crary Trough, which we attribute to displacement upon high angle faults. Portions of basin-bounding faults were previously detected by ground-based gravity surveys upon the Whillans Ice Stream flank (Figure 4a, Muto et al., 2013) and site J9DC (Figure 3b), where large variations in sediment thickness indicate up to 600m of fault throw (Greischar et al., 1992). The continuity between the narrow Siple Dome Basin (this study) and the Trunk D Basin (Figure 3a, Bell et al., 2006) suggests that the active tectonic domain continues southward past the GZ. The fault-controlled tectonic basins may reflect a crustal response to the lithospheric foundering hypothesized beneath the South Pole region (Shen, Wiens, Stern, et al., 2018) or be a broader regional expression of Neogene extension that formed the Bentley Subglacial Trench (Lloyd et al., 2015).

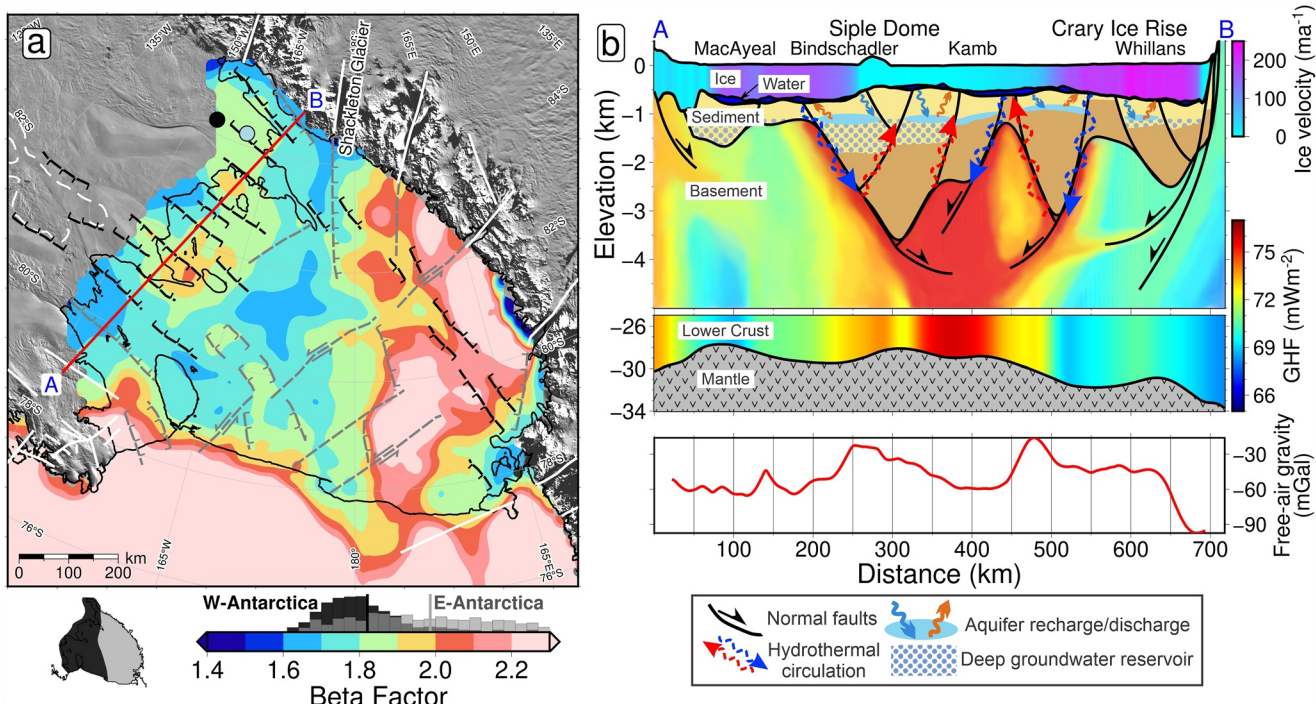


Figure 4. Tectonic interpretation of the sub-Ross Ice Shelf. (a) β stretching factors (Text S6 in Supporting Information S1). Colorbar histogram shows data distribution of West versus East Antarctic sides, same as Figure 3. Black and gray lines indicate inferred active and inactive faults, respectively, with kinematics shown with half-arrows (strike or oblique-slip) and hachures (normal-sense). White lines show previously reported faults, same as Figure 3a. Dashed-white outline is Trunk D Basin (Bell et al., 2006). Black and blue dots show Subglacial Lake Whillans and sedimentary basin from Gustafson et al. (2022), respectively. Cross-section A-B in red. (b) Siple Coast cross-section from A-B, showing basin sediments bounded by faults, with geothermal heat flux through the crust (lower panel from Burton-Johnson et al. (2020), upper panel interpreted). Ice surface, ice base, and bathymetry from Morlighem et al. (2020). Ice streams colored by velocity (Mouginot et al., 2019; Venturelli et al., 2020). Moho is from Shen, Wiens, Anandakrishnan, et al. (2018). Lower panel shows ROSETTA-Ice gravity. Named features are labeled on top.

4.2. Consequences for Ice Sheet Dynamics

Our basement topography and suggested crustal faults likely exert a strong influence on the overriding ice, especially along the Siple Coast. Here, we show deep and thick sedimentary basins which likely contain voluminous basinal aquifers (Figure 4b; cf. Gustafson et al., 2022). Where these aquifers discharge along fault-damage zones, they can enhance GHF and promote basal melting (Gooch et al., 2016), as depicted in Figure 4a. The elevated GHF seen at Subglacial Lake Whillans (285 mW/m², Fisher et al., 2015) may arise from fault localization (Figure 4a). Confinement of the aquifers between the ice bed and low-permeability basement may promote fluid overpressure, enabling ice streaming (e.g., Ravier & Buoncristiani, 2018). Additionally, the Siple Coast faults likely accommodate the solid Earth's response to fluctuating ice volume. A matter receiving considerable debate (Lowry et al., 2019; Neuhaus et al., 2021; Venturelli et al., 2020), is Kingslake et al.'s (2018) finding of rapid re-advance of the Siple Coast GZ following Holocene deglaciation. The re-advance was in part due to swift glacioisostatic rebound (cf. Coulon et al., 2021; Lowry et al., 2020), a process aided by the region's low-viscosity mantle (Whitehouse et al., 2019) and likely to be accommodated upon pre-existing crustal faults, as observed in the Lambert Graben (Phillips & Läufer, 2009). Our proposed graben-bounding faults would provide a tectonic control on the glacioisostatic adjustment of the Siple Coast region.

4.3. Mid-Shelf High - Central High

The 650-km-long Mid-Shelf High features three shallow, blocky segments >150 km in breadth, which have only thin sediment cover (<200m). At their shallowest points, the top of basement lies within ~300m of the ice shelf base, at a depth comparable to the basement high at Roosevelt Island. Roosevelt Island is a modern pinning point (Still et al., 2019) owing to the thicker sediment, there (Figure 3b). We introduce the MSH as a prominent pinning point at times of advance and greater extent of the Antarctic Ice Sheet, in keeping with evidence from subglacial sediment records that indicate a major ice flow divide between East and West Antarctic ice during and since Last Glacial Maximum (Coenen et al., 2019; X. Li et al., 2020; Licht et al., 2014).

The prominence of the MSH is due in part to the contrasting geologic properties of the East versus West Antarctic type crust and their respective responses to WARS extension. We distinguished β -factors on the TAM-side that are high and uniform, indicating distributed crustal extension. The West Antarctic side displays lower β -factors overall, but with localized extreme thinning beneath Siple Coast (Figure 4a). The greater amount of extension on the East Antarctic side coincides with the deeper bathymetry (Figure 1a), deeper basement, and thicker sediments (Figure 3). The contrasting properties are also evident in ROSETTA-Ice magnetic and gravity anomalies, used by Tinto et al. (2019) to identify a north-south trending tectonic boundary along the midline of Ross Embayment. The MSH in the magnetic basement coincides with and spans this boundary, which has been further substantiated by passive-seismic studies that show a lithospheric-scale boundary (Cheng et al., 2021; White-Gaynor et al., 2019). To the north, the features continue into the Ross Sea's CH. Southward, the MSH basement feature trends into the TAM, where its western edge aligns with Shackleton Glacier, occupying a major fault separating the distinct geologic domains of the central and southern TAM (Borg et al., 1990; Paulsen et al., 2004), which also parallels a prominent magnetic lineament at the South Pole (Studinger et al., 2006). The structure may be an expression of the East Antarctic craton margin or a major intracontinental transform (Figure 4a, Studinger et al., 2006).

At the time of Oligocene initiation of the Antarctic Ice sheet, paleotopographic reconstructions of the proto-Ross Embayment depict a long, broad range, emergent above sea level (Paxman et al., 2019; Wilson et al., 2012), that we equate to the MSH-CH that divides the Embayment. The CH hosted small ice caps with alpine glaciers formed during the initial glacial stage in the region (De Santis et al., 1995), and continental ice expanded to the outer Ross Sea continental shelf from those centers (Bart & De Santis, 2012). Between the late Oligocene and mid-Miocene, the CH subsided by up to 500m (Kulhanek et al., 2019; Leckie, 1983), receiving 100's of meters of sediment cover (~400m at DSDP 270; De Santis et al., 1995). The geophysical similarities and continuity between the Ross Sea's CH and the RIS's MSH imply a similar glaciation and subsidence history for the MSH. A terrestrial/alpine stage for the MSH helps to explain the region's potential to hold the late Oligocene's larger-than-modern ice volumes (Pekar et al., 2006; Wilson et al., 2013), with the MSH-CH having a central role in Oligocene ice sheet development and the subsequent evolution of the ice sheet and ice shelf, as is documented in the Ross Sea (Halberstadt et al., 2016).

4.4. Thermal Subsidence and Sedimentation

Incorporating the updated basement basin extents and geometries into post-rift thermal subsidence modeling will enable better constrained paleotopographic reconstructions. For the sub-RIS, these reconstructions (Paxman et al., 2019; Wilson et al., 2012) use a post-Eocene subsidence model based on gravity-derived basin geometries and uniform β -factors (Wilson & Luyendyk, 2009). This model predicts uniform stretching of the eastern sub-RIS from the ice front to the Siple Coast, while our β -factors show increasing stretching from the ice front to the Siple Coast. This observed additional thinning likely has resulted in more subsidence for Siple Dome and the north flank of Crary Ice Rise, which can now be accounted for in reconstructions. Our sediment thickness comparison with past models (Text S6 in Supporting Information S1, Wilson & Luyendyk, 2009) shows the majority of the sub-RIS, especially the Siple Coast, contains more total sediment than previously estimated (Figure S1f in Supporting Information S1). Depending on the age of this sediment, reconstructions may need to account for the additional sediment deposition and loading.

5. Conclusions

Here we present a depth to magnetic basement map for the RIS from Werner deconvolution of airborne magnetic data. The RIS magnetic basement is tied to Ross Sea seismic basement, providing the first synthetic view of Ross Embayment crustal structure. Using a bathymetry model, we obtain the sediment thickness distribution and calculate crustal extension factors for the sub-RIS. The extensional features we image, resulting from West Antarctic Rift System extension, have continuity with Ross Sea basement structures to the north, and the prominent Mid-Shelf High trends northward into the Ross Sea's CH. This combined high separates East and West Antarctic type crust, affected by different degrees of continental extension. The Mid-Shelf High was likely subaerial in the Oligocene, able to support alpine ice caps in early Antarctic glaciation. Subsequently it formed a prominent pinning point and ice flow divide between the East and West Antarctic Ice Sheets.

Newly identified narrow, linear, deep sedimentary basins provide evidence of active faults beneath the Siple Coast GZ, where thinned crust overlying anomalous mantle (Shen, Wiens, Anandakrishnan, et al., 2018) likely experiences elevated geothermal heat flow promoting the formation of subglacial water. Faults that control basement margins may accommodate motion caused by the glacioisostatic response to ice sheet volume changes. Subglacial sedimentary basins in this setting likely contain confined aquifers within permeable basin fill. Here, ice overburden pressure would control flow both between and within the subglacial and groundwater systems, possibly localizing geothermal heat. Updated sediment thickness and basin extents should be incorporated into new paleotopographic reconstructions of time intervals of interest for paleo-ice sheet modeling. Our work contributes critical information about Ross Embayment basement topography and subglacial boundary conditions that arise from an interplay of geology, tectonics, and glaciation.

Data Availability Statement

ROSETTA-Ice and Operation IceBridge magnetics data are available through <https://www.usap-dc.org/view/project/p0010035> and <https://nsidc.org/data/IMCS31b>, respectively. Results from this study are available to download from <https://doi.pangaea.de/10.1594/PANGAEA.941238> and a Jupyter notebook documenting our workflow and figure creation is available at <https://zenodo.org/badge/latestdoi/470814953>.

References

- An, M., Wiens, D. A., Zhao, Y., Feng, M., Nyblade, A. A., Kanao, M., et al. (2015). S-velocity model and inferred Moho topography beneath the Antarctic Plate from Rayleigh waves: Antarctic S-velocities and Moho. *Journal of Geophysical Research: Solid Earth*, 120(1), 359–383. <https://doi.org/10.1002/2014JB011332>
- Austermann, J., Pollard, D., Mitrovica, J. X., Moucha, R., Forte, A. M., DeConto, R. M., et al. (2015). The impact of dynamic topography change on Antarctic ice sheet stability during the mid-Pliocene warm period. *Geology*, 43(10), 927–930. <https://doi.org/10.1130/G36988.1>
- Bart, P., & De Santis, L. (2012). Glacial intensification during the Neogene: A review of seismic stratigraphic evidence from the Ross Sea, Antarctica, continental shelf. *Oceanography*, 25(3), 166–183. <https://doi.org/10.5670/oceanog.2012.92>
- Beaudoin, B. C., ten Brink, U. S., & Stern, T. A. (1992). Characteristics and processing of seismic data collected on thick, floating ice: Results from the Ross Ice Shelf, Antarctica. *Geophysics*, 57(10), 1359–1372. <https://doi.org/10.1190/1.1443205>
- Begeman, C. B., Tulaczyk, S. M., & Fisher, A. T. (2017). Spatially variable geothermal heat flux in West Antarctica: Evidence and implications. *Geophysical Research Letters*, 44(19), 9823–9832. <https://doi.org/10.1002/2017GL075579>

- Bell, R. E., Ferraccioli, F., Creyts, T. T., Braaten, D., Corr, H., Das, I., et al. (2011). Widespread persistent thickening of the East Antarctic Ice Sheet by freezing from the base. *Science*, 331(6024), 1592–1595. <https://doi.org/10.1126/science.1200109>
- Bell, R. E., Studinger, M., Karner, G., Finn, C. A., & Blankenship, D. D. (2006). Identifying major sedimentary basins beneath the West Antarctic Ice Sheet from aeromagnetic data analysis. In D. K. Fütterer, D. Damaske, G. Kleinschmidt, H. Miller, & F. Tessensohn (Eds.), *Antarctica* (pp. 117–121). Springer-Verlag. https://doi.org/10.1007/3-540-32934-X_13
- Borg, S. G., Depaolo, D. J., & Smith, B. M. (1990). Isotopic structure and tectonics of the central Transantarctic Mountains. *Journal of Geophysical Research*, 95(B5), 6647. <https://doi.org/10.1029/JB095iB05p06647>
- Brancolini, G., Busetti, M., Marchetti, A., Santis, L. D., Zanolla, C., Cooper, A. K., & Hinze, K. (1995). Descriptive text for the seismic stratigraphic atlas of the Ross Sea, Antarctica. In A. K. Cooper, P. F. Barker, & G. Brancolini (Eds.), *Geology and Seismic Stratigraphy of the Antarctic Margin*. (Vol. 68, pp. A271–A286). American Geophysical Union. <https://doi.org/10.1002/9781118669013.app1>
- Burton-Johnson, A., Dziadek, R., & Martin, C. (2020). Geothermal heat flow in Antarctica: Current and future directions. *The Cryosphere Discussions*, 1–45. <https://doi.org/10.5194/tc-2020-59>
- Cheng, W., Hu, X. G., & Liu, L. T. (2021). Anisotropy gradients in the middle of the Ross Sea Embayment, West Antarctica: Evidence from QL scattered surface waves. *Geophysical Research Letters*, 48(6), e2020GL091232. <https://doi.org/10.1029/2020GL091232>
- Chiappini, M., Ferraccioli, F., Bozzo, E., & Damaske, D. (2002). Regional compilation and analysis of aeromagnetic anomalies for the Transantarctic Mountains–Ross Sea sector of the Antarctic. *Tectonophysics*, 347(1–3), 121–137. [https://doi.org/10.1016/S0040-1951\(01\)00241-4](https://doi.org/10.1016/S0040-1951(01)00241-4)
- Christoffersen, P., Bougamont, M., Carter, S. P., Fricker, H. A., & Tulaczyk, S. (2014). Significant groundwater contribution to Antarctic ice streams hydrologic budget. *Geophysical Research Letters*, 41(6), 2003–2010. <https://doi.org/10.1002/2014GL059250>
- Cochran, J. R., Burton, B., Frearson, N., & Tinto, K. (2014). *IceBridge Scintrex CS-3 Cesium magnetometer LIB geolocated magnetic anomalies*. version 2. [Line 403, 404]. NASA National Snow and Ice Data Center Distributed Active Archive Center. <https://doi.org/10.5067/OY7C2Y61YSYW>
- Coenen, J. J., Scherer, R. P., Baudoin, P., Warny, S., Castañeda, I. S., & Askin, R. (2019). Paleogene marine and terrestrial development of the West Antarctic Rift System. *Geophysical Research Letters*, 47(3), e2019GL085281. <https://doi.org/10.1029/2019GL085281>
- Colleoni, F., De Santis, L., Montoli, E., Olivo, E., Sorlien, C. C., Bart, P. J., et al. (2018). Past continental shelf evolution increased Antarctic Ice Sheet sensitivity to climatic conditions. *Scientific Reports*, 8(1), 11323. <https://doi.org/10.1038/s41598-018-29718-7>
- Cooper, A. K., Barker, P. F., & Brancolini, G. (Eds.). (1995). *Geology and Seismic Stratigraphy of the Antarctic Margin*. AGU. (Vol. 68). <https://doi.org/10.1029/AR068>
- Coulon, V., Bulthuis, K., Whitehouse, P. L., Sun, S., Haubner, K., Zipf, L., & Pattyn, F. (2021). Contrasting response of West and East Antarctic Ice Sheets to glacial isostatic adjustment. *Journal of Geophysical Research: Earth Surface*, 126(7), e2020JF006003. <https://doi.org/10.1029/2020JF006003>
- DeConto, R. M., & Pollard, D. (2003). A coupled climate–Ice Sheet modeling approach to the Early Cenozoic history of the Antarctic Ice Sheet. *Palaeogeography, Palaeoclimatology, Palaeoecology*, 198(1–2), 39–52. [https://doi.org/10.1016/S0031-0182\(03\)00393-6](https://doi.org/10.1016/S0031-0182(03)00393-6)
- De Santis, L., Anderson, J. B., Brancolini, G., & Zayatz, I. (1995). Seismic record of late Oligocene through Miocene glaciation on the central and eastern continental shelf of the Ross Sea. In A. K. Cooper, P. F. Barker, & G. Brancolini (Eds.), *Antarctic research series* (pp. 235–260). American Geophysical Union. <https://doi.org/10.1029/AR068p0235>
- Drenth, B. J., Grauch, V., Turner, K. J., Rodriguez, B. D., Thompson, R. A., & Bauer, P. W. (2019). A shallow rift basin segmented in space and time: The southern San Luis Basin, Rio Grande rift, northern New Mexico, U.S.A. *Rocky Mountain Geology*, 54(2), 97–131. <https://doi.org/10.2487/rmgjournal.54.2.97>
- Ferraccioli, F., Bozzo, E., & Damaske, D. (2002). Aeromagnetic signatures over Western Marie Byrd Land provide insight into magmatic arc basement, mafic magmatism and structure of the Eastern Ross Sea Rift flank. *Tectonophysics*, 347(1–3), 139–165. [https://doi.org/10.1016/S0040-1951\(01\)00242-6](https://doi.org/10.1016/S0040-1951(01)00242-6)
- Finn, C. (2002). *Examples of the utility of magnetic anomaly data for geologic mapping (Open-File Report No. 02-400)*. USGS.
- Fisher, A. T., Mankoff, K. D., Tulaczyk, S. M., Tyler, S. W., Foley, N., & The WISSARD Science Team. (2015). High geothermal heat flux measured below the West Antarctic Ice Sheet. *Science Advances*, 1(6), 1–9. <https://doi.org/10.1126/sciadv.1500093>
- Ford, A., & Barrett, P. J. (1975). *Basement rocks of the south-central Ross Sea, site 270, DSDP leg 28 (Tech. Rep.)*. Texas A & M University, Ocean Drilling Program. <https://doi.org/10.2973/dsdp.proc.28.130.1975>
- Frederick, B. C., Young, D. A., Blankenship, D. D., Richter, T. G., Kempf, S. D., Ferraccioli, F., & Siegert, M. J. (2016). Distribution of subglacial sediments across the Wilkes Subglacial Basin, East Antarctica. *Journal of Geophysical Research: Earth Surface*, 121(4), 790–813. <https://doi.org/10.1002/2015JF003760>
- Gooch, B. T., Young, D. A., & Blankenship, D. D. (2016). Potential groundwater and heterogeneous heat source contributions to ice sheet dynamics in critical submarine basins of East Antarctica. *Geochemistry, Geophysics, Geosystems*, 17(2), 395–409. <https://doi.org/10.1002/2015GC006117>
- Goodge, J. W. (2020). Geological and tectonic evolution of the Transantarctic Mountains, from ancient craton to recent enigma. *Gondwana Research*, 80, 50–122. <https://doi.org/10.1016/j.gr.2019.11.001>
- Granot, R., & Dymnt, J. (2018). Late Cenozoic unification of East and West Antarctica. *Nature Communications*, 9(1), 3189. <https://doi.org/10.1038/s41467-018-05270-w>
- Greischar, L. L., Bentley, C. R., & Whiting, L. R. (1992). An analysis of gravity measurements on the Ross Ice Shelf, Antarctica. In *Contributions to Antarctic research III* (pp. 105–155). American Geophysical Union (AGU). <https://doi.org/10.1029/AR057p0105>
- Gustafson, C. D., Key, K., Siegfried, M. R., Winberry, J. P., Fricker, H. A., Venturelli, R. A., & Michaud, A. B. (2022). A dynamic saline ground-water system mapped beneath an Antarctic ice stream. *Science*, 376(6593), 640–644. <https://doi.org/10.1126/science.abm3301>
- Halberstadt, A. R. W., Simkins, L. M., Greenwood, S. L., & Anderson, J. B. (2016). Past ice-sheet behaviour: Retreat scenarios and changing controls in the Ross Sea, Antarctica. *The Cryosphere*, 10(3), 1003–1020. <https://doi.org/10.5194/tc-10-1003-2016>
- Jolie, E., Scott, S., Faulds, J., Chambefort, I., Axelsson, G., Gutiérrez-Negrín, L. C., et al. (2021). Geological controls on geothermal resources for power generation. *Nature Reviews Earth & Environment*, 2(5), 324–339. <https://doi.org/10.1038/s43017-021-00154-y>
- Jordan, T. A., Riley, T. R., & Siddoway, C. S. (2020). The geological history and evolution of West Antarctica. *Nature Reviews Earth & Environment*, 1(2), 117–133. <https://doi.org/10.1038/s43017-019-0013-6>
- Karner, G. D., Studinger, M., & Bell, R. E. (2005). Gravity anomalies of sedimentary basins and their mechanical implications: Application to the Ross Sea basins, West Antarctica. *Earth and Planetary Science Letters*, 235(3–4), 577–596. <https://doi.org/10.1016/j.epsl.2005.04.016>
- Kingslake, J., Scherer, R. P., Albrecht, T., Coenen, J., Powell, R. D., Reese, R., et al. (2018). Extensive retreat and re-advance of the West Antarctic Ice Sheet during the Holocene. *Nature*, 558(7710), 430–434. <https://doi.org/10.1038/s41586-018-0208-x>
- Kulhanek, D. K., Levy, R. H., Clowes, C. D., Preble, J. G., Rodelli, D., Jovane, L., et al. (2019). Revised chronostratigraphy of DSDP Site 270 and late Oligocene to early Miocene paleoecology of the Ross Sea sector of Antarctica. *Global and Planetary Change*, 178, 46–64. <https://doi.org/10.1016/j.gloplacha.2019.04.002>

- Leckie, F. M. (1983). Late Oligocene-early Miocene glacial record of the Ross Sea, Antarctica: Evidence from DSDP Site 270. *Geology*, 11, 578–582. [https://doi.org/10.1130/0091-7613\(1983\)11<578:LOMGRO>2.0.CO;2](https://doi.org/10.1130/0091-7613(1983)11<578:LOMGRO>2.0.CO;2)
- Li, L., Aitken, A., Lindsay, M., & Kulessa, B. (2021). Subglacial sedimentary basins focus key vulnerabilities of the Antarctic Ice-Sheet (Preprint). *Review*. <https://doi.org/10.21203/rs.3.rs-1117673/v1>
- Li, X., Zatlin, M., & Olivetti, V. (2020). Apatite fission track signatures of the Ross Sea ice flows during the Last Glacial Maximum. *Geochemistry, Geophysics, Geosystems*, 21(10), 1–21. <https://doi.org/10.1029/2019GC008749>
- Licht, K. J., Hennessy, A. J., & Welke, B. M. (2014). The U-Pb detrital zircon signature of West Antarctic ice stream tills in the Ross embayment, with implications for Last Glacial Maximum ice flow reconstructions. *Antarctic Science*, 26(6), 687–697. <https://doi.org/10.1017/S0954102014000315>
- Lloyd, A. J., Wiens, D. A., Nyblade, A. A., Anandakrishnan, S., Aster, R. C., Huerta, A. D., et al. (2015). A seismic transect across West Antarctica: Evidence for mantle thermal anomalies beneath the Bentley Subglacial Trench and the Marie Byrd Land Dome. *Journal of Geophysical Research: Solid Earth*, 120(12), 8439–8460. <https://doi.org/10.1002/2015JB012455>
- Lowry, D. P., Golledge, N. R., Bertler, N. A., Jones, R. S., McKay, R., & Stutz, J. (2020). Geologic controls on ice sheet sensitivity to deglacial climate forcing in the Ross Embayment, Antarctica. *Quaternary Science Advances*, 1, 1–17. <https://doi.org/10.1016/j.qsa.2020.100002>
- Lowry, D. P., Golledge, N. R., Bertler, N. A. N., Jones, R. S., & McKay, R. (2019). Deglacial grounding-line retreat in the Ross Embayment, Antarctica, controlled by ocean and atmosphere forcing. *Science Advances*, 5(8), 1–12. <https://doi.org/10.1126/sciadv.aav8754>
- Luyendyk, B., Sorlien, C. C., Wilson, D. S., Bartek, L. R., & Siddoway, C. S. (2001). Structural and tectonic evolution of the Ross Sea rift in the Cape Colbeck region, Eastern Ross Sea, Antarctica. *Tectonics*, 20(6), 933–958. <https://doi.org/10.1029/2000TC001260>
- Luyendyk, B., Wilson, D. S., & Siddoway, C. S. (2003). Eastern margin of the Ross Sea Rift in Western Marie Byrd Land, Antarctica: Crustal structure and tectonic development. *Geochemistry, Geophysics, Geosystems*, 4(10), 1–25. <https://doi.org/10.1029/2002GC000462>
- Morlighem, M., Rignot, E., Binder, T., Blankenship, D., Drews, R., Eagles, G., et al. (2020). Deep glacial troughs and stabilizing ridges unveiled beneath the margins of the Antarctic Ice Sheet. *Nature Geoscience*, 13(2), 132–137. <https://doi.org/10.1038/s41561-019-0510-8>
- Mouginot, J., Rignot, E., & Scheuchl, B. (2019). Continent-wide, interferometric SAR phase, mapping of Antarctic ice velocity. *Geophysical Research Letters*, 46(16), 9710–9718. <https://doi.org/10.1029/2019GL083826>
- Müller, R. D., Gohl, K., Cande, S. C., Goncharov, A., & Golynsky, A. V. (2007). Eocene to Miocene geometry of the West Antarctic Rift System. *Australian Journal of Earth Sciences*, 54(8), 1033–1045. <https://doi.org/10.1080/08120090701615691>
- Muto, A., Christianson, K., Horgan, H. J., Anandakrishnan, S., & Alley, R. B. (2013). Bathymetry and geological structures beneath the Ross Ice Shelf at the mouth of Whillans Ice Stream, West Antarctica, modeled from ground-based gravity measurements. *Journal of Geophysical Research: Solid Earth*, 118(8), 4535–4546. <https://doi.org/10.1002/jgrb.50315>
- Neuhaus, S. U., Tulaczyk, S. M., Stansell, N. D., Coenen, J. J., Scherer, R. P., Mikucki, J. A., & Powell, R. D. (2021). Did Holocene climate changes drive West Antarctic grounding line retreat and readvance? *The Cryosphere*, 15(10), 4655–4673. <https://doi.org/10.5194/tc-15-4655-2021>
- Paulsen, T., Encarnación, J., & Grunow, A. (2004). Structure and timing of transpressional deformation in the Shackleton Glacier area, Ross orogen, Antarctica. *Journal of the Geological Society*, 161(6), 1027–1038. <https://doi.org/10.1144/0016-764903-040>
- Paxman, G. J. G., Jamieson, S. S., Hochmuth, K., Gohl, K., Bentley, M. J., Leitchenkov, G., & Ferraccioli, F. (2019). Reconstructions of Antarctic topography since the Eocene–Oligocene boundary. *Palaeogeography, Palaeoclimatology, Palaeoecology*, 535, 109346. <https://doi.org/10.1016/j.palaeo.2019.109346>
- Pekar, S. F., DeConto, R. M., & Harwood, D. M. (2006). Resolving a late Oligocene conundrum: Deep-sea warming and Antarctic glaciation. *Palaeogeography, Palaeoclimatology, Palaeoecology*, 231(1–2), 29–40. <https://doi.org/10.1016/j.palaeo.2005.07.024>
- Pérez, L. F., De Santis, L., McKay, R. M., Larter, R. D., Ash, J., Bart, P. J., et al. (2021). Early and middle Miocene ice sheet dynamics in the Ross Sea: Results from integrated core-log-seismic interpretation. *GSA Bulletin*, 134(1–2), 348–370. <https://doi.org/10.1130/B35814.1>
- Phillips, G., & Läufer, A. (2009). Brittle deformation relating to the Carboniferous–Cretaceous evolution of the Lambert Graben, East Antarctica: A precursor for Cenozoic relief development in an intraplate and glaciated region. *Tectonophysics*, 471(3–4), 216–224. <https://doi.org/10.1016/j.tecto.2009.02.012>
- Ravier, E., & Buoncristiani, J.-F. (2018). Glaciohydrogeology. In *Past glacial environments* (pp. 431–466). Elsevier. <https://doi.org/10.1016/B978-0-08-100524-8.00013-0>
- Rignot, E., Jacobs, S., Mouginot, J., & Scheuchl, B. (2013). Ice-shelf melting around Antarctica. *Science*, 341(6143), 266–270. <https://doi.org/10.1126/science.1235798>
- Salvini, F., Brancolini, G., Busetti, M., Storti, F., Mazzarini, F., & Coren, F. (1997). Cenozoic geodynamics of the Ross Sea region, Antarctica: Crustal extension, intraplate strike-slip faulting, and tectonic inheritance. *Journal of Geophysical Research*, 102(B11), 24669–24696. <https://doi.org/10.1029/97JB01643>
- Sauli, C., Sorlien, C., Busetti, M., De Santis, L., Geletti, R., Wardell, N., & Luyendyk, B. P. (2021). Neogene development of the Terror Rift, Western Ross Sea, Antarctica. *Geochemistry, Geophysics, Geosystems*, 22(3). <https://doi.org/10.1029/2020GC009076>
- Scambos, T., Haran, T., Fahnestock, M., Painter, T., & Bohlander, J. (2007). MODIS-based Mosaic of Antarctica (MOA) data sets: Continent-wide surface morphology and snow grain size. *Remote Sensing of Environment*, 111(2–3), 242–257. <https://doi.org/10.1016/j.rse.2006.12.020>
- Shen, W., Wiens, D. A., Anandakrishnan, S., Aster, R. C., Gerstoft, P., Bromirski, P. D., et al. (2018). The crust and upper mantle structure of Central and West Antarctica from Bayesian inversion of Rayleigh wave and receiver functions. *Journal of Geophysical Research: Solid Earth*, 123(9), 7824–7849. <https://doi.org/10.1029/2017JB015346>
- Shen, W., Wiens, D. A., Stern, T., Anandakrishnan, S., Aster, R. C., Dalziel, I., et al. (2018). Seismic evidence for lithospheric foundering beneath the southern Transantarctic Mountains, Antarctica. *Geology*, 46(1), 71–74. <https://doi.org/10.1130/G39555.1>
- Siddoway, C. S. (2008). Tectonics of the West Antarctic Rift System: New light on the history and dynamics of distributed intracontinental extension. In A. K. Cooper, et al. (Eds.). In *Antarctica: A keystone in a changing world*. The National Academies Press. <https://doi.org/10.3133/ofr20071047KP09>
- Siegert, M. J., Kulessa, B., Bougamont, M., Christoffersen, P., Key, K., Andersen, K. R., et al. (2018). Antarctic subglacial groundwater: A concept paper on its measurement and potential influence on ice flow. *Geological Society, London, Special Publications*, 461(1), 197–213. <https://doi.org/10.1144/SP461.8>
- Sorlien, C. C., Luyendyk, B., Wilson, D. S., Decesari, R. C., Bartek, L. R., & Diebold, J. B. (2007). Oligocene development of the West Antarctic Ice Sheet recorded in eastern Ross Sea strata. *Geology*, 35(5), 467. <https://doi.org/10.1130/G23387A.1>
- Stern, T. A., Davey, F. J., & Delisle, G. (1991). Lithospheric flexure induced by the load of the Ross Archipelago, southern Victoria land, Antarctica. In M. Thomson, A. Crame, & J. Thomson (Eds.), *Geological evolution of Antarctica* (pp. 323–328). Cambridge University Press.
- Still, H., Campbell, A., & Hulbe, C. (2019). Mechanical analysis of pinning points in the Ross Ice Shelf, Antarctica. *Annals of Glaciology*, 60(78), 32–41. <https://doi.org/10.1017/aog.2018.31>

- Studinger, M., Bell, R., Fitzgerald, P., & Buck, W. (2006). Crustal architecture of the Transantarctic Mountains between the Scott and Reedy Glacier region and South Pole from aerogeophysical data. *Earth and Planetary Science Letters*, 250(1–2), 182–199. <https://doi.org/10.1016/j.epsl.2006.07.035>
- Studinger, M., Bell, R. E., Buck, W., Karner, G. D., & Blankenship, D. D. (2004). Sub-ice geology inland of the Transantarctic Mountains in light of new aerogeophysical data. *Earth and Planetary Science Letters*, 220(3–4), 391–408. [https://doi.org/10.1016/S0012-821X\(04\)00066-4](https://doi.org/10.1016/S0012-821X(04)00066-4)
- Ten Brink, U. S., Bannister, S., Beaudoin, B. C., & Stern, T. A. (1993). Geophysical investigations of the tectonic boundary between East and West Antarctica. *Science*, 261(5117), 45–50. <https://doi.org/10.1126/science.261.5117.45>
- Tinto, K. J., Padman, L., Siddoway, C. S., Springer, S. R., Fricker, H. A., Das, I., et al. (2019). Ross Ice Shelf response to climate driven by the tectonic imprint on seafloor bathymetry. *Nature Geoscience*, 12(6), 441–449. <https://doi.org/10.1038/s41561-019-0370-2>
- Uieda, L., Tian, D., Leong, W. J., Jones, M., Schlitzer, W., Toney, L., et al. (2021). PyGMT: A Python interface for the Generic Mapping Tools. *Zenodo*. <https://doi.org/10.5281/zenodo.5607255>
- Venturelli, R. A., Siegfried, M. R., Roush, K. A., Li, W., Burnett, J., Zook, R., et al. (2020). Mid-Holocene grounding line retreat and readvance at Whillans Ice Stream, West Antarctica. *Geophysical Research Letters*, 47(15), e2020GL088476. <https://doi.org/10.1029/2020GL088476>
- Werner, S. (1953). Interpretation of magnetic anomalies at sheet-like bodies. In *Sveriges geologiska undersök* (pp. 413–449).
- Wessel, P., Luis, J. F., Uieda, L., Scharroo, R., Wobbe, F., Smith, W. H. F., & Tian, D. (2019). The generic mapping tools version 6. *Geochemistry, Geophysics, Geosystems*, 20(11), 5556–5564. <https://doi.org/10.1029/2019GC008515>
- White-Gaynor, A. L., Nyblade, A. A., Aster, R. C., Wiens, D. A., Bromirski, P. D., Gerstoft, P., et al. (2019). Heterogeneous upper mantle structure beneath the Ross Sea Embayment and Marie Byrd Land, West Antarctica, revealed by P-wave tomography. *Earth and Planetary Science Letters*, 513, 40–50. <https://doi.org/10.1016/j.epsl.2019.02.013>
- Whitehouse, P. L., Gomez, N., King, M. A., & Wiens, D. A. (2019). Solid Earth change and the evolution of the Antarctic Ice Sheet. *Nature Communications*, 10(1), 503. <https://doi.org/10.1038/s41467-018-08068-y>
- Wilson, D. S., Jamieson, S. S., Barrett, P. J., Leitchenkov, G., Gohl, K., & Larer, R. D. (2012). Antarctic topography at the Eocene–Oligocene boundary. *Palaeogeography, Palaeoclimatology, Palaeoecology*, 335–336, 24–34. <https://doi.org/10.1016/j.palaeo.2011.05.028>
- Wilson, D. S., & Luyendyk, B. (2009). West Antarctic paleotopography estimated at the Eocene-Oligocene climate transition. *Geophysical Research Letters*, 36(16), L16302. <https://doi.org/10.1029/2009GL039297>
- Wilson, D. S., Pollard, D., DeConto, R. M., Jamieson, S. S., & Luyendyk, B. (2013). Initiation of the West Antarctic Ice Sheet and estimates of total Antarctic ice volume in the earliest Oligocene. *Geophysical Research Letters*, 40(16), 4305–4309. <https://doi.org/10.1002/grl.50797>
- Zhou, Z., Wiens, D. A., Shen, W., Aster, R. C., Nyblade, A., & Wilson, T. J. (2022). Radial Anisotropy and sediment thickness of West and Central Antarctica estimated from Rayleigh and Love wave velocities. *Journal of Geophysical Research: Solid Earth*, 127(3). <https://doi.org/10.1029/2021JB022857>

References From the Supporting Information

- Andrews, J. T., & LeMasurier, W. (2021). Resolving the argument about volcanic bedrock under the West Antarctic Ice Sheet and implications for ice sheet stability and sea level change. *Earth and Planetary Science Letters*, 568, 117035. <https://doi.org/10.1016/j.epsl.2021.117035>
- Cox, S., Smith Lytle, B., & the GeoMAP team (2019). SCAR GeoMAP dataset. *GNS Science*. <https://doi.org/10.21420/7SH7-6K05>
- Crary, A. P. (1961). Marine-sediment thickness in the eastern Ross Sea area, Antarctica. *The Geological Society of America Bulletin*, 72, 7872. <https://doi.org/10.1130/0016-7606%281961%2972%25B787%25MTITER%25D2.0.CO%3F>
- Fretwell, P., Pritchard, H. D., Vaughan, D. G., Bamber, J. L., Barrand, N. E., Bell, R. E., et al. (2013). Bedmap2: Improved ice bed, surface and thickness datasets for Antarctica. *The Cryosphere*, 7(1), 375–393. <https://doi.org/10.5194/tc-7-375-2013>
- Lindeque, A., Gohl, K., Wobbe, F., & Uenzelmann-Neben, G. (2016). Preglacial to glacial sediment thickness grids for the Southern Pacific Margin of West Antarctica: Preglacial, transitional and full glacial isopach maps, West Antarctica. *Geochemistry, Geophysics, Geosystems*, 17(10), 4276–4285. <https://doi.org/10.1002/2016GC006401>
- Mooney, W. D., Laske, G., & Masters, T. G. (1998). Crust 5.1: A global crustal model at 5° × 5°. *Journal of Geophysical Research*, 103(B1), 727–747. <https://doi.org/10.1029/97JB02122>
- Robertson, J. D., & Bentley, C. R. (1989). The Ross Ice Shelf: Glaciology and geophysics paper 3: Seismic studies on the grid Western half of the Ross Ice Shelf: RIGGS I and RIGGS II. In C. R. Bentley & D. E. Hayes (Eds.), *Antarctic Research Series*, (Vol. 42, pp. 55–86). American Geophysical Union. <https://doi.org/10.1029/AR042p0055>
- Rooney, S. T., Blankenship, D. D., & Bentley, C. R. (1987). Seismic refraction measurements of crustal structure in West Antarctica. In G. D. Mckenzie (Ed.), *Geophysical monograph series* (pp. 1–7). American Geophysical Union. <https://doi.org/10.1029/GM040p0001>
- Smith, W. H. F., & Wessel, P. (1990). Gridding with continuous curvature splines in tension. *Geophysics*, 55(3), 293–305. <https://doi.org/10.1190/1.1442837>